Supp.Fig 1

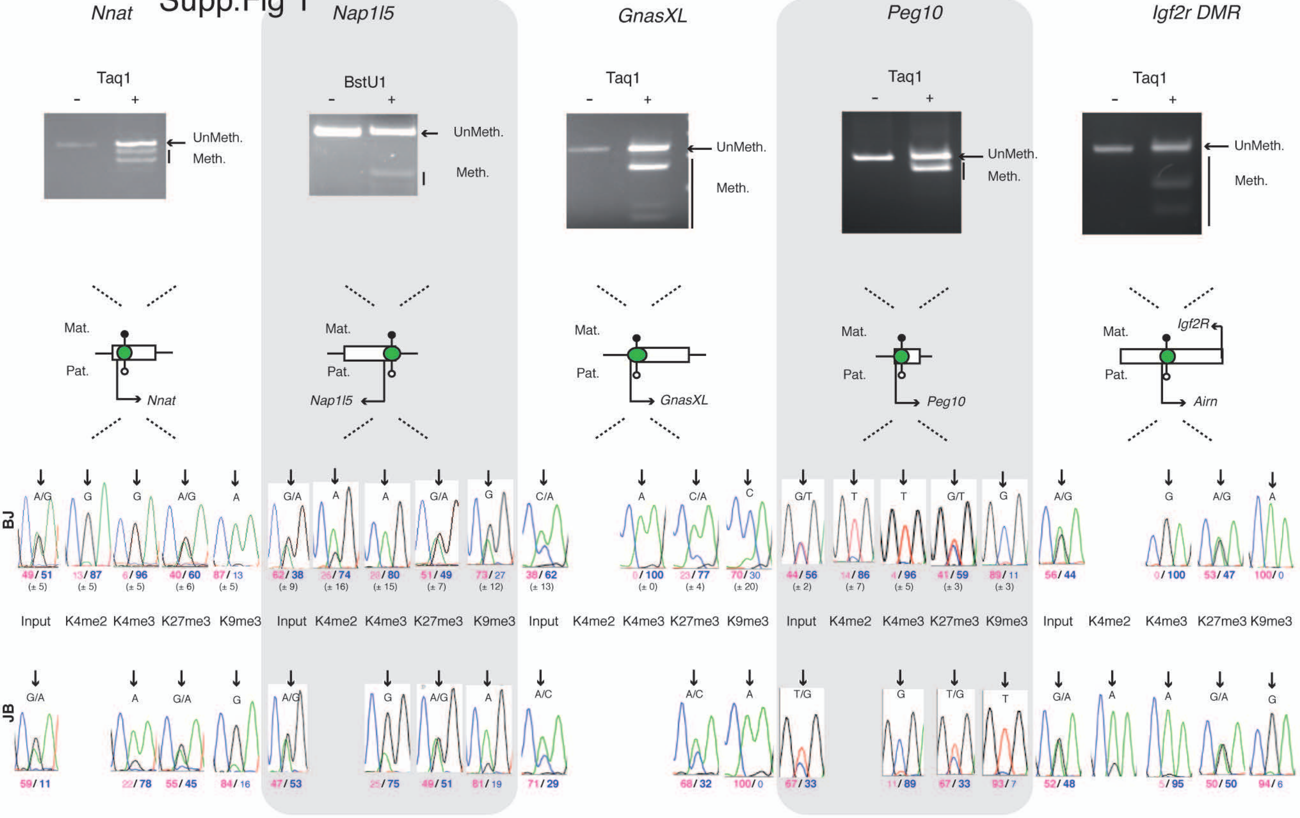
Nnat
Nap1l5
GnasXL
Peg10
Igf2r DMR
Taq1
-
+
UnMeth.
Meth.
BstU1
-
+
UnMeth.
Meth.
Taq1
-
+
UnMeth.
Meth.
Taq1
-
+
UnMeth.
Meth.
Taq1
-
+
UnMeth.
Meth.
Mat.
Pat.
Nnat
Mat.
Pat.
Nap1l5
Mat.
Pat.
GnasXL
Mat.
Pat.
Peg10
Mat.
Igf2R
Pat.
Airn
BJ
A/G
G
G
A/G
A
49/51 (± 5)
13/87 (± 5)
6/96 (± 5)
40/60 (± 6)
87/13 (± 5)
G/A
A
A
G/A
G
62/38 (± 9)
26/74 (± 16)
28/80 (± 15)
51/49 (± 7)
73/27 (± 12)
C/A
A
C/A
C
38/62 (± 13)
0/100 (± 0)
23/77 (± 4)
70/30 (± 20)
G/T
T
T
G/T
G
44/56 (± 2)
14/86 (± 7)
4/96 (± 5)
41/59 (± 3)
89/11 (± 3)
A/G
G
A/G
A
56/44
0/100
53/47
100/0
Input K4me2 K4me3 K27me3 K9me3
Input K4me2 K4me3 K27me3 K9me3
Input K4me2 K4me3 K27me3 K9me3
Input K4me2 K4me3 K27me3 K9me3
Input K4me2 K4me3 K27me3 K9me3
JB
G/A
A
G/A
G
59/11
22/78
55/45
84/16
A/G
G
A/G
A
47/53
25/75
49/51
81/19
A/C
A/C
A
71/29
68/32
100/0
T/G
G
T/G
T
67/33
11/89
67/33
93/7
G/A
A
A
G/A
G
52/48
5/95
50/50
94/6

Supplementary Figure S1: Maternal ICRs associated with bivalent chromatin in ES cells

Schematic showing the analyzed ICRs (green circles) and their relative position relative to the main associated gene(s). The DNA methylation pattern is symbolized by lollipops (black: methylated; white: unmethylated) and the name of the transcripts initiating from the ICR region is also indicated. The upper panels show representative data obtained by the bisulfite-based approach COBRA in BJ1 ES cells for each ICR. The enzyme used for the digestion and the expected position of the obtained methylated (Meth.) and unmethylated (UnMeth.) digestion products are indicated.

The lower panels show data obtained following native ChIP with anti-H3-K4me2,-K4me3, -K27me3 and -K9me3 antibodies. The allelic distribution of each mark was determined by direct sequencing of the PCR product encompassing a strain-specific SNP in the analyzed region. Representative data obtained in BJ1 and JB1 ES cells are shown. The mean values (± standard deviation) of the relative allelic ratios (Pink: maternal; Blue: paternal) are indicated. All these ICRs are marked by a bivalent domain on their paternal unmethylated allele in ES cells.

Supp.Fig 2

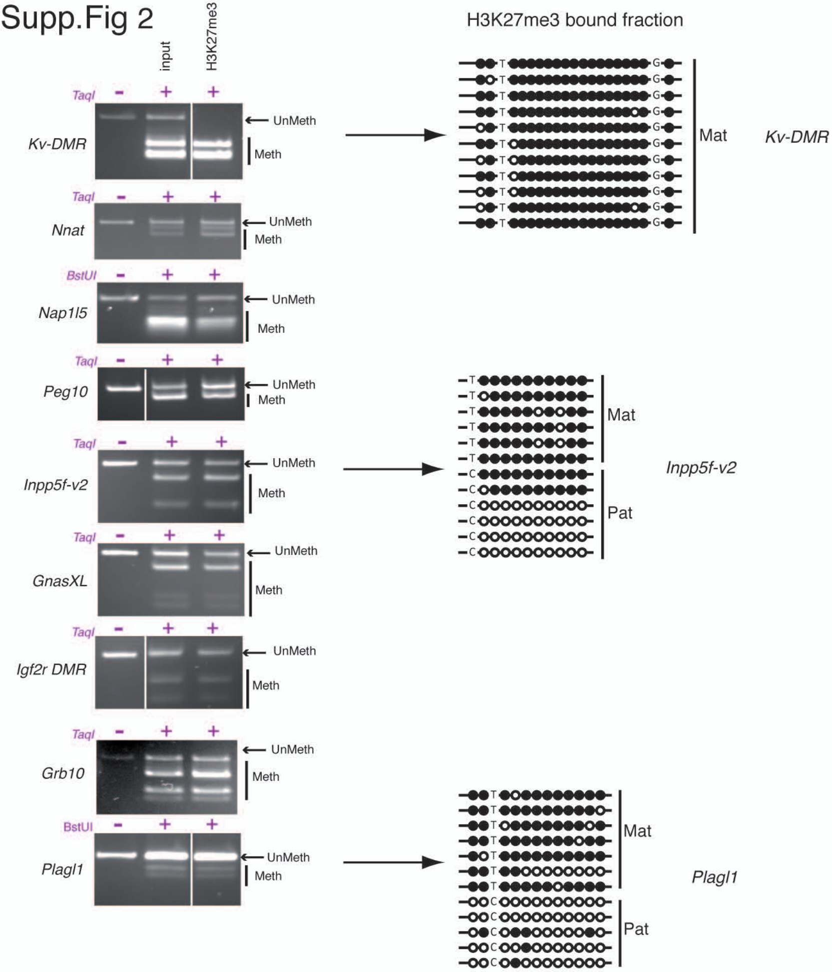
input
H3K27me3
H3K27me3 bound fraction
TaqI
Kv-DMR
UnMeth
Meth
Nnat
BstUI
Nap1l5
Peg10
Inpp5f-v2
GnasXL
Igf2r DMR
Grb10
Plagl1
Mat
Pat
Kv-DMR
Inpp5f-v2
Plagl1

Supplementary Figure S2: H3K27me3 and DNA methylation co-exist on the same parental allele at a subset of mat-ICRs

Bisulfite-based DNA methylation analysis of H3K27me3-bound chromatin and the associated input at several mat-ICRs in BJ1 ES cells. The COBRA-based (left panels) approach and direct sequencing (right panels) show that H3K27me3 is associated with the methylated allele at *Kv-DMR* and with both the methylated and unmethylated alleles at “bivalent chromatin associated-ICRs”.

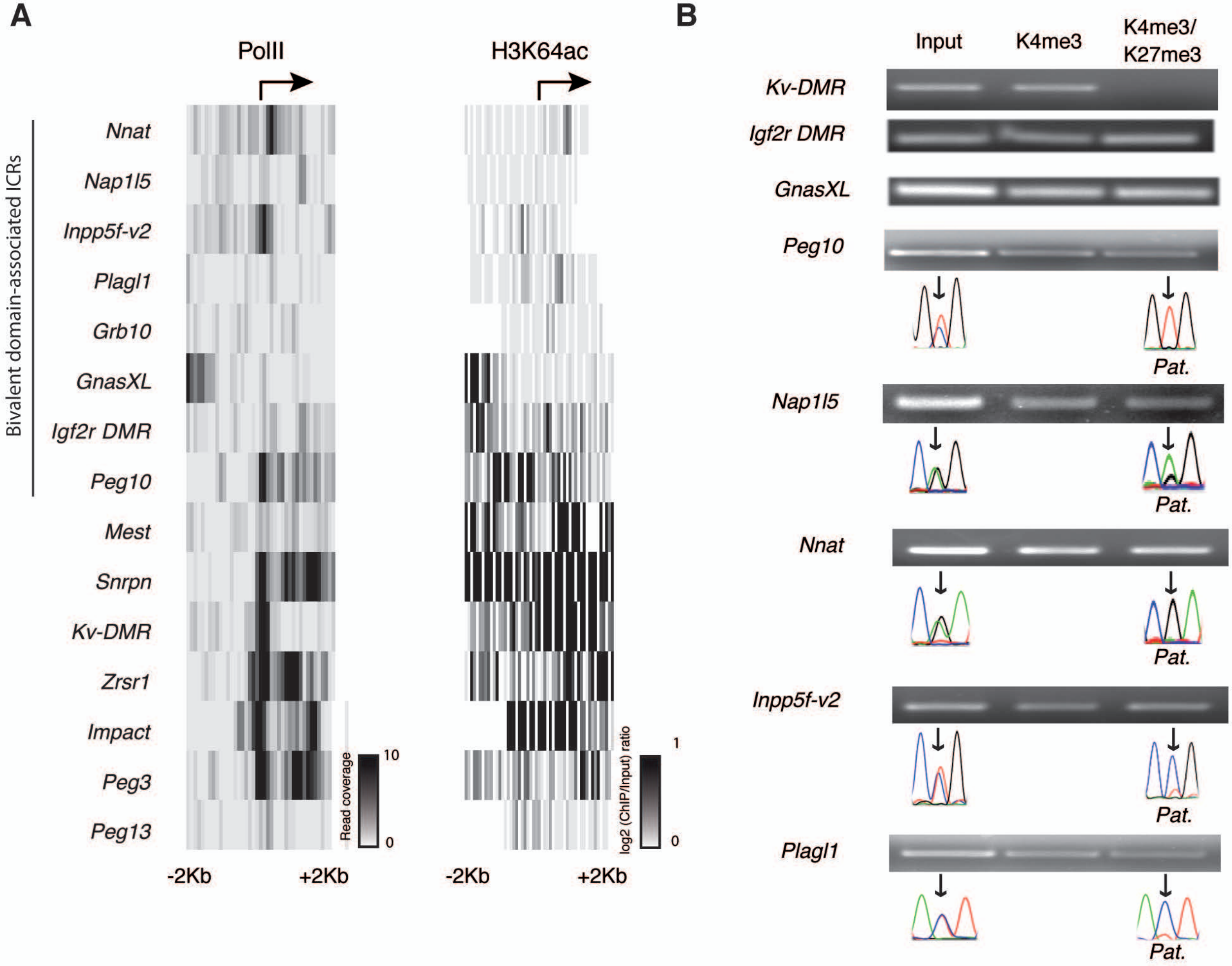

Supp. Figure 3

Supplementary Figure S3: Characterization of mat-ICRs marked by bivalent chromatin in ES cells

A) Enrichment for total PolII and H3K64ac at mat-ICRs. For each promoter/ICR, enrichment is shown in a 4Kb window centered on the TSS. Raw data were extracted from publicly available ChIP-seq data (replicate samples GSM1173371/GSM1173372 for total PolII (Bunch et al., 2014) and replicate samples GSM866724/ GSM866723 for H3K64ac (Di Cerbo et al., 2014)) and processed with a home-made script.

B) Representative data obtained following sequential ChIP with anti-H3K4me3 and then -H3K27me3 antibodies. Sequencing of the immunoprecipitated material obtained in the second round of precipitation shows that these two marks are enriched on the same paternal chromatin fragments. *Kv-DMR* is shown as a negative control.

Supp.Fig 4A

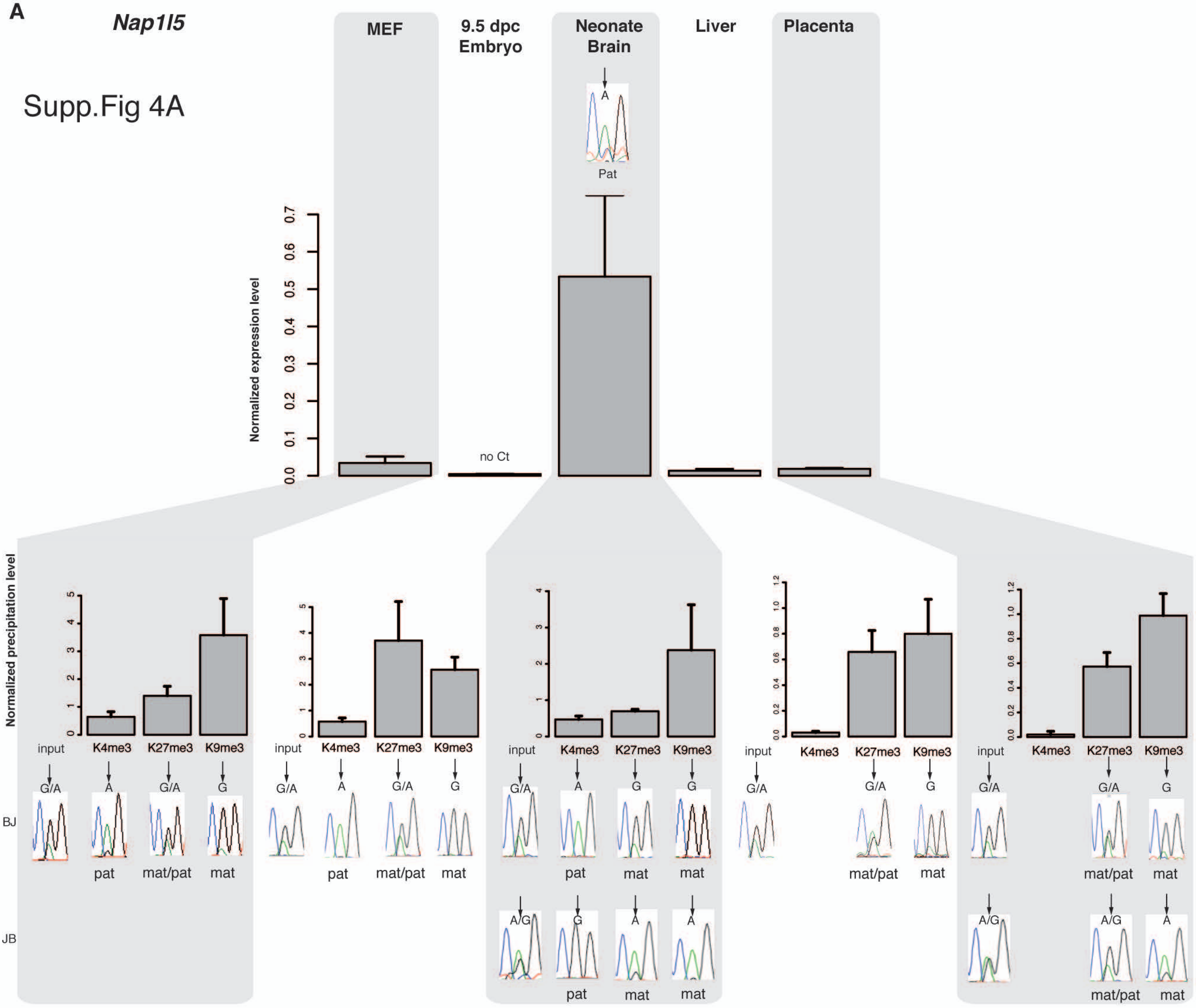
A
Nap1l5
MEF
9.5 dpc Embryo
Neonate Brain
Liver
Placenta
A
Pat
Normalized expression level
0.0
0.1
0.2
0.3
0.4
0.5
0.6
0.7
no Ct
Normalized precipitation level
input
K4me3
K27me3
K9me3
G/A
A
G
A/G
BJ
JB
pat
mat/pat
mat

Supp.Fig 4B

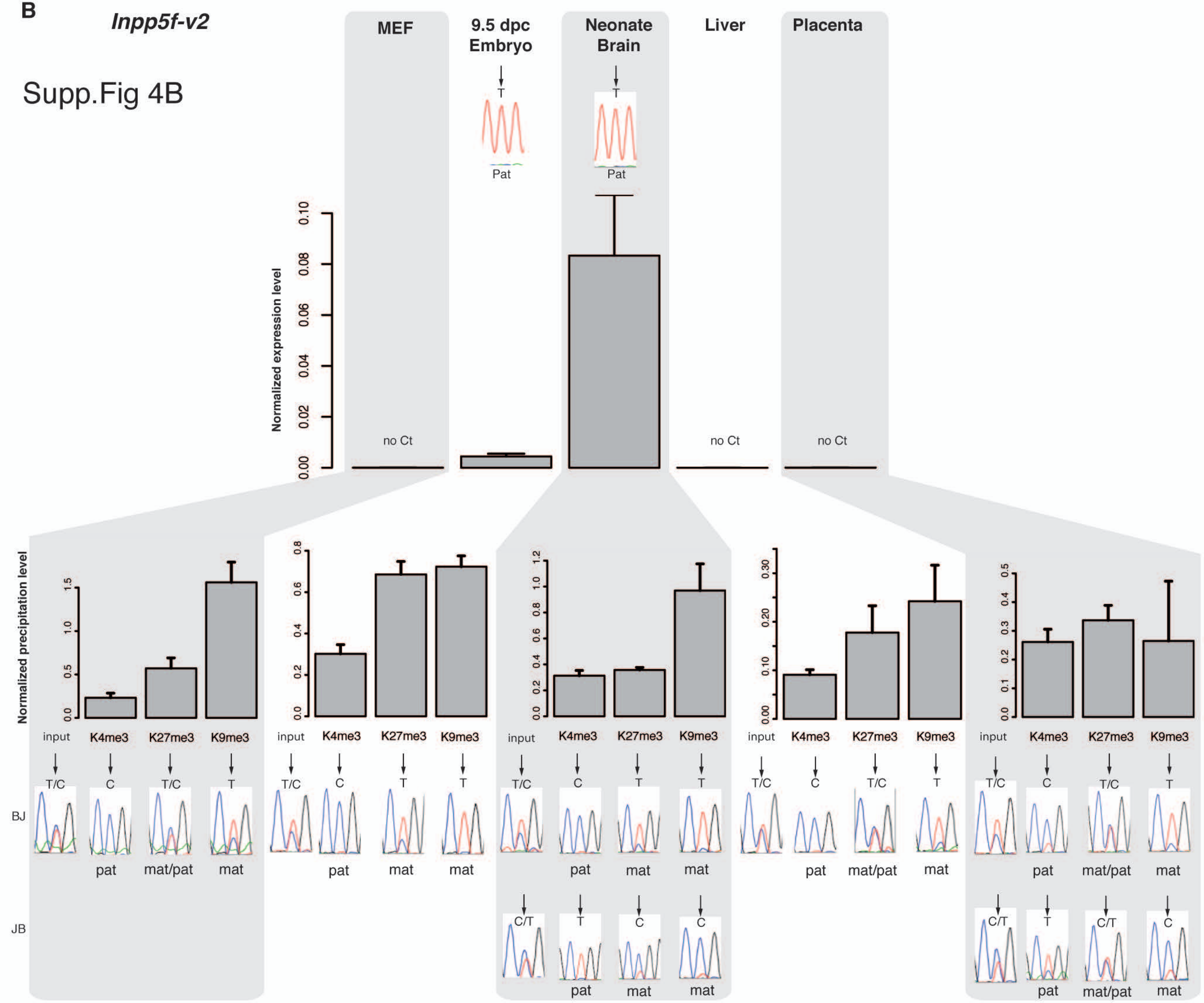
B
Inpp5f-v2
MEF
9.5 dpc Embryo
Neonate Brain
Liver
Placenta
T
Pat
T
Pat
Normalized expression level
0.00
0.02
0.04
0.06
0.08
0.10
no Ct
no Ct
no Ct
Normalized precipitation level
0.0
0.5
1.0
1.5
0.0
0.2
0.4
0.6
0.8
0.0
0.2
0.4
0.6
0.8
1.0
1.2
0.00
0.10
0.20
0.30
0.0
0.1
0.2
0.3
0.4
0.5
input
K4me3
K27me3
K9me3
BJ
JB
T/C
C
T
C/T
pat
mat/pat
mat

Supp.Fig 4C

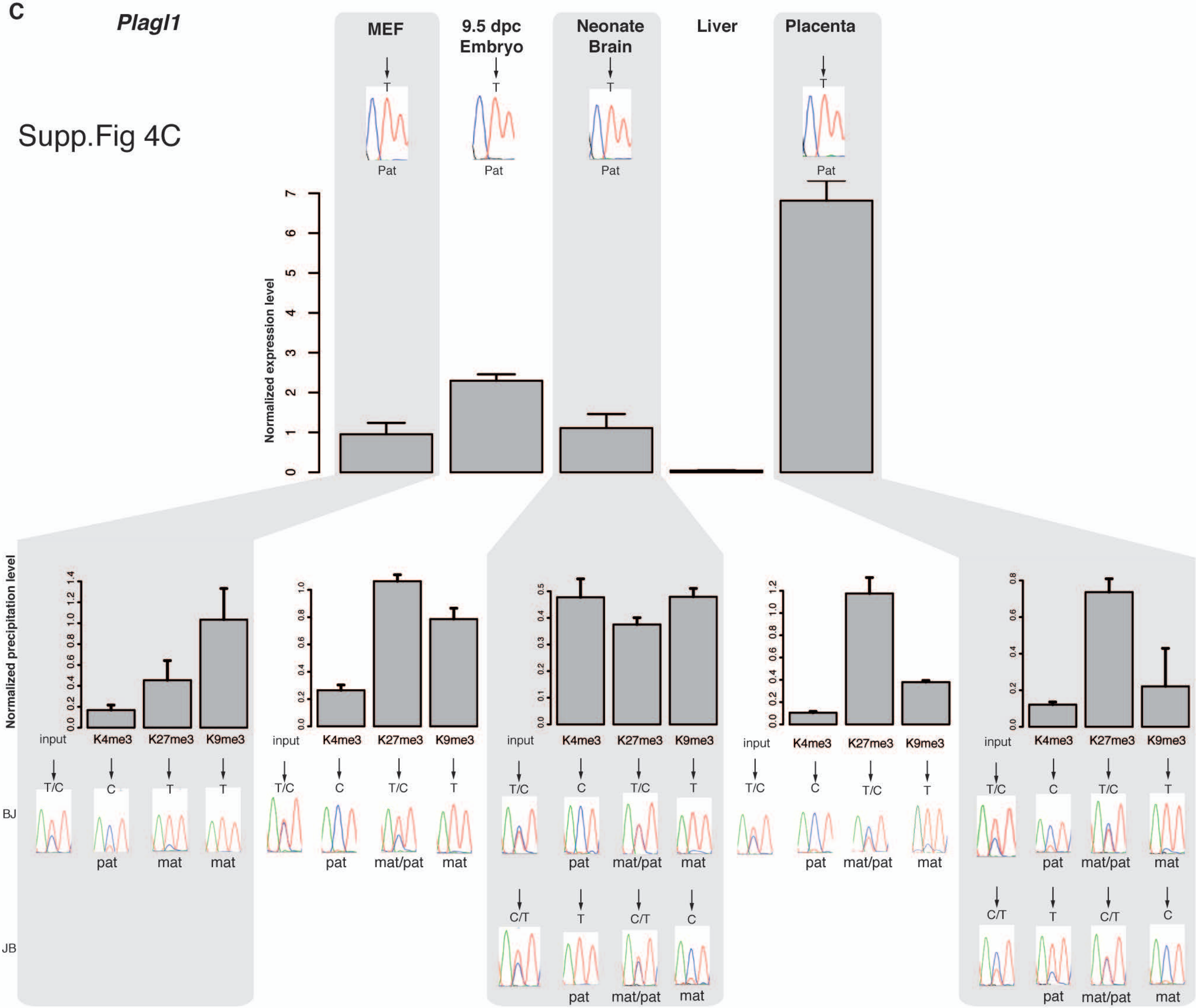
C
Plagl1
MEF
9.5 dpc Embryo
Neonate Brain
Liver
Placenta
T
Pat
Normalized expression level
0
1
2
3
4
5
6
7
Normalized precipitation level
input
K4me3
K27me3
K9me3
BJ
JB
T/C
C
T
C/T
pat
mat
mat/pat
0.0
0.2
0.4
0.6
0.8
1.0
1.2
1.4
0.1
0.3
0.5

Supplementary Figure S4: Paternal expression correlates with loss of H3K27me3 at mat-ICRs marked by bivalent chromatin

Representative results obtained at the *Nap1l5* (A), *Inpp5f-v2* (B) and *Plagl1*(C) ICRs.

The upper panel shows the gene expression analyses in a panel of C57Bl6/JF1 (BJ) samples. Results were normalized to the expression level of the two housekeeping genes *Ppia* and *Rpl30*. For each sample, analyses were repeated four times, each in duplicate. The parental origin of expression was determined by direct sequencing of the PCR product encompassing a strain-specific SNP in the analyzed region. The lower panels show the chromatin analysis following native ChIP with anti-H3-K4me3, -K27me3 and –K9me3 antibodies. The precipitation level was normalized to that obtained at the *Rpl30* promoter (for H3K4me3), the *HoxA3* or *HoxD8* promoter (for H3K27me3) and *IAP* (for H3K9me3). For each tissue, the value is reported as the mean of at least three independent ChIP experiments (n), each analyzed in duplicate: MEFs (n=3); E9.5 embryos (n=3); neonate brain (BJ n=2; JB n=2); liver (n=3); placenta (BJ n=2; JB n=1). The allelic distribution of these marks was determined by direct sequencing of the PCR product encompassing a strain-specific SNP in the analyzed region.

Supp.Fig 5

Kv-DMR

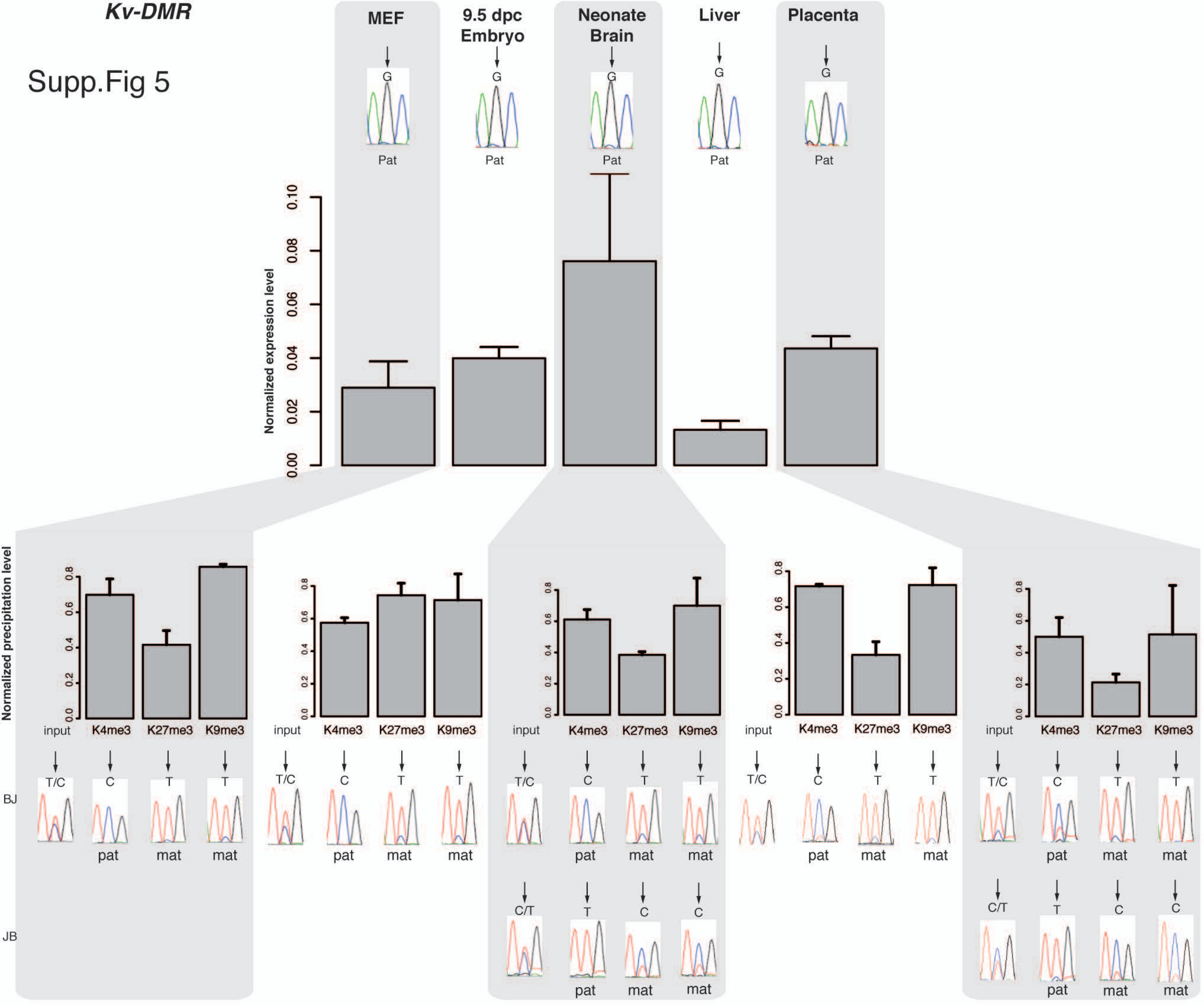

Supplementary Figure S5: ICRs with ubiquitous promoter activity have a canonical chromatin signature.

Kv-DMR is shown as an example of a ubiquitously active promoter/ICR. The upper panel shows the expression analysis in a panel of BJ samples. Results were normalized to the expression level of the housekeeping genes *Ppia* and *Rpl30*. For each sample type, the analysis was repeated four times, each in duplicate. The parental origin of expression was determined by direct sequencing of the PCR product encompassing a strain-specific SNP in the analyzed region.

The lower panels show the chromatin analysis following native ChIP against H3-K4me3, -K27me3 and –K9me3. The precipitation level was normalized to that obtained at the *Rpl30* promoter for H3K4me3, the *HoxA3* or *HoxD8* promoter for H3K27me3, and *IAP* for H3K9me3. For each sample type, the value is reported as the mean of at least three independent ChIP experiments (n), each in duplicate: MEFs (n=3); 9.5dpc embryos (n=3); neonate brain (B/J n=2; J/B n=2); liver (n=3); placenta (BJ n=2; JB n=1). The parental origin of expression and the allelic distribution of each mark were determined by direct sequencing of the PCR product encompassing a strain-specific SNP in the analyzed region.

Supp.Fig 6

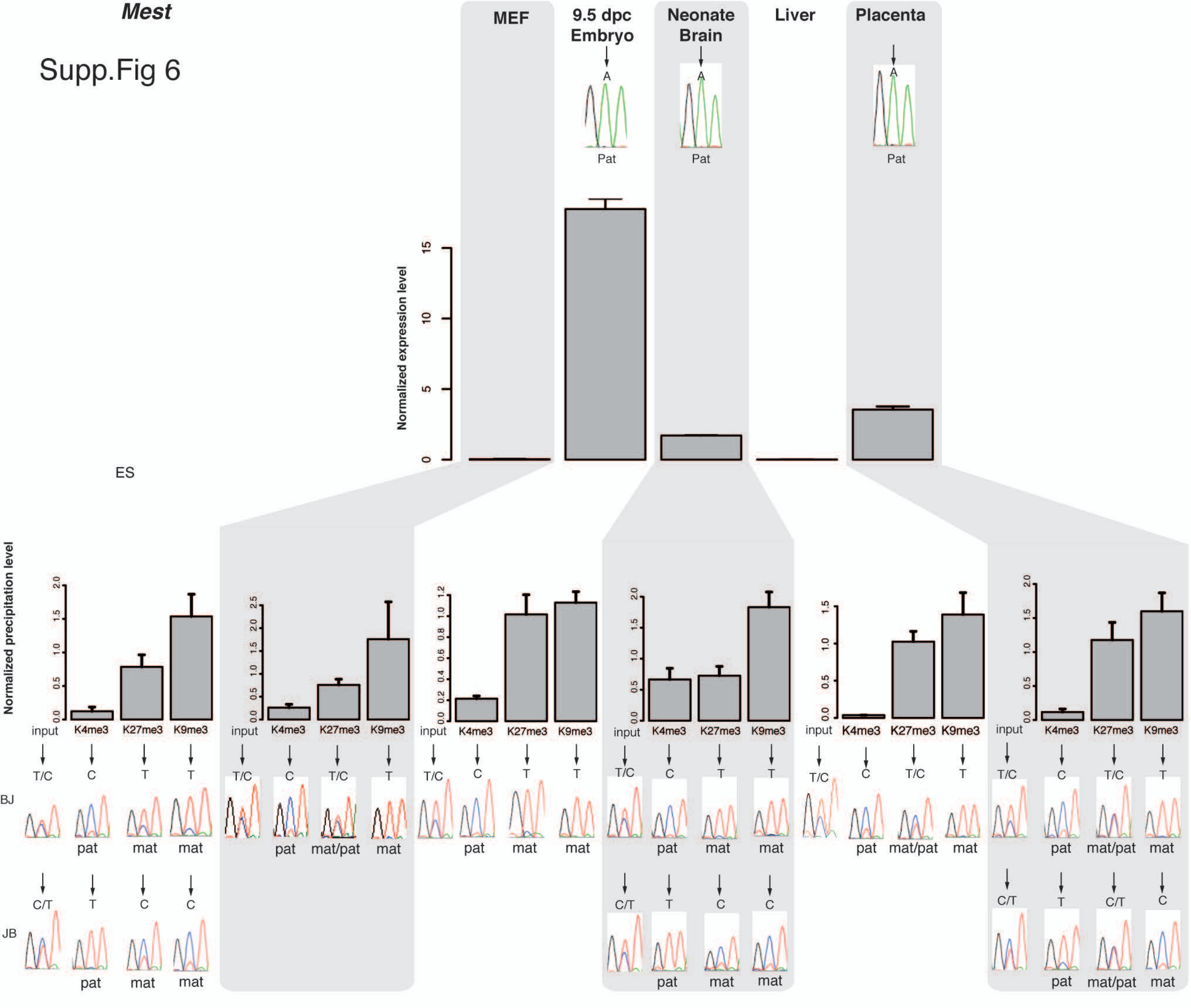
Mest
MEF
9.5 dpc Embryo
Neonate Brain
Liver
Placenta
A
Pat
A
Pat
A
Pat
Normalized expression level
0
5
10
15
ES
Normalized precipitation level
input
K4me3
K27me3
K9me3
T/C
C
T
T
pat
mat
mat
BJ
C/T
T
C
C
pat
mat
mat
JB
T/C
C
T/C
T
pat
mat/pat
mat
T/C
C
T
T
pat
mat
mat
T/C
C
T
T
pat
mat
mat
C/T
T
C
C
pat
mat
mat
T/C
C
T/C
T
pat
mat/pat
mat
T/C
C
T/C
T
pat
mat/pat
mat
C/T
T
C/T
C
pat
mat/pat
mat
0.0
0.5
1.0
1.5
2.0
2.5
0.2
0.4
0.6
0.8
1.2

Supplementary Figure S6: The *Mest* ICR gains bivalent chromatin in non-expressing tissues.

Gene expression and chromatin analyses at the *Mest* ICR. Details of the legend are as in supplementary Figure S5. At this ICR, chromatin bivalency is absent in ES cells and is gained, through acquisition of H3K27me3 on the paternal allele in non-expressing tissues/MEFs. Note that, as observed at the *Plagl1* ICR (Figure E4C), bivalency is maintained on the paternal allele in placenta despite expression, suggesting that the detected expression arise from a subpopulation of cells within this tissue.

Supp.Fig 7

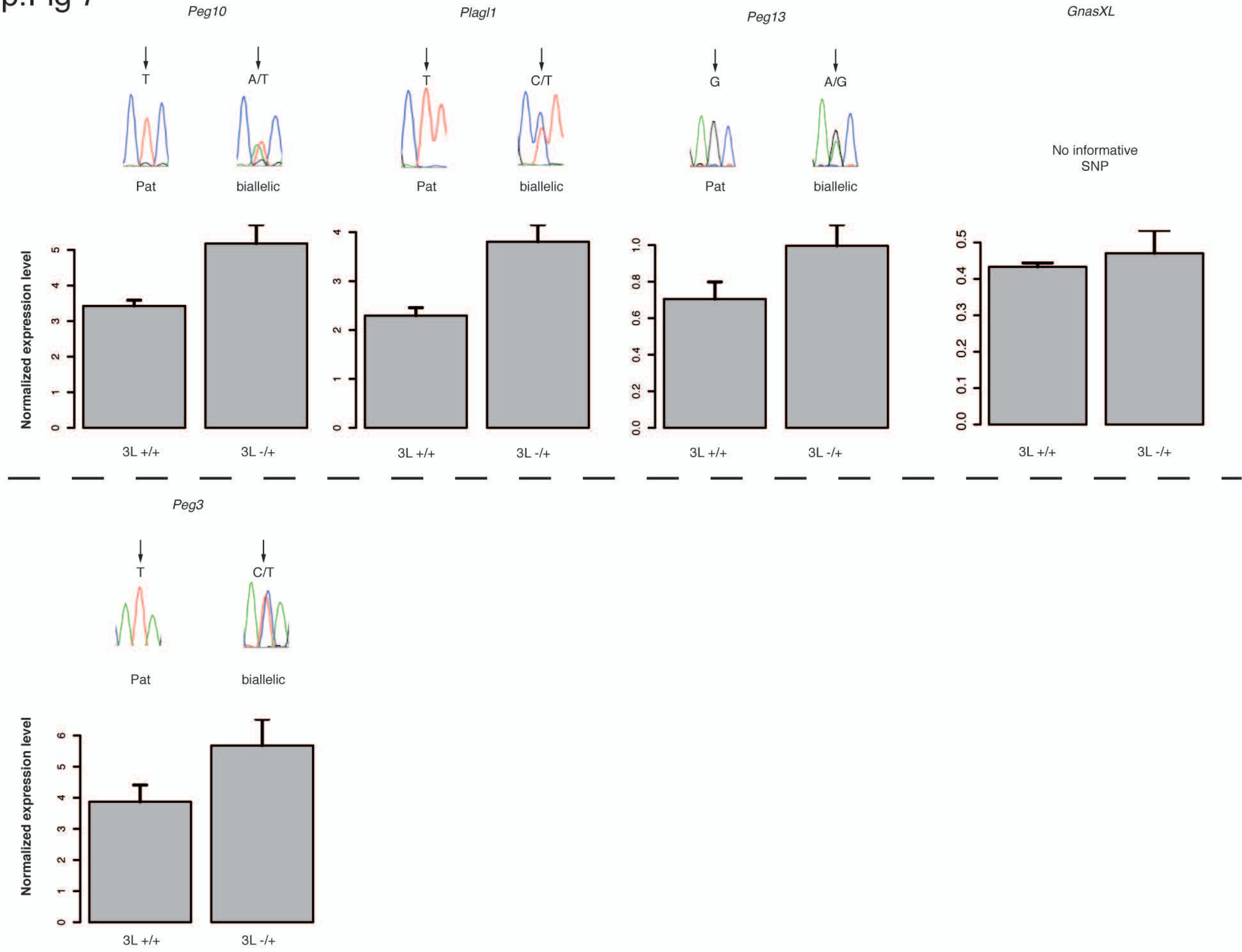
Peg10
T
A/T
Pat
biallelic
Normalized expression level
0
1
2
3
4
5
3L +/+
3L -/+
Plagl1
T
C/T
Pat
biallelic
0
1
2
3
4
3L +/+
3L -/+
Peg13
G
A/G
Pat
biallelic
0.0
0.2
0.4
0.6
0.8
1.0
3L +/+
3L -/+
GnasXL
No informative SNP
0.0
0.1
0.2
0.3
0.4
0.5
3L +/+
3L -/+
Peg3
T
C/T
Pat
biallelic
Normalized expression level
0
1
2
3
4
5
6
3L +/+
3L -/+

Supplementary Figure S7: Most ICR-associated transcripts are expressed biallelicaly in *Dnmt3l*$^{-/+}$ embryos

Example of gene expression analysis in pools of at least 15 WT and *Dnmt3l*$^{-/+}$ E9.5 embryos. Results are presented as the percentage of the geometrical mean of the expression of *Ppia* and *Rpl30*. Data were obtained from two independent experiments, each in duplicate. The parental origin of expression at the indicated ICRs was determined by direct sequencing of the PCR product encompassing a strain-specific SNP in the analyzed region.

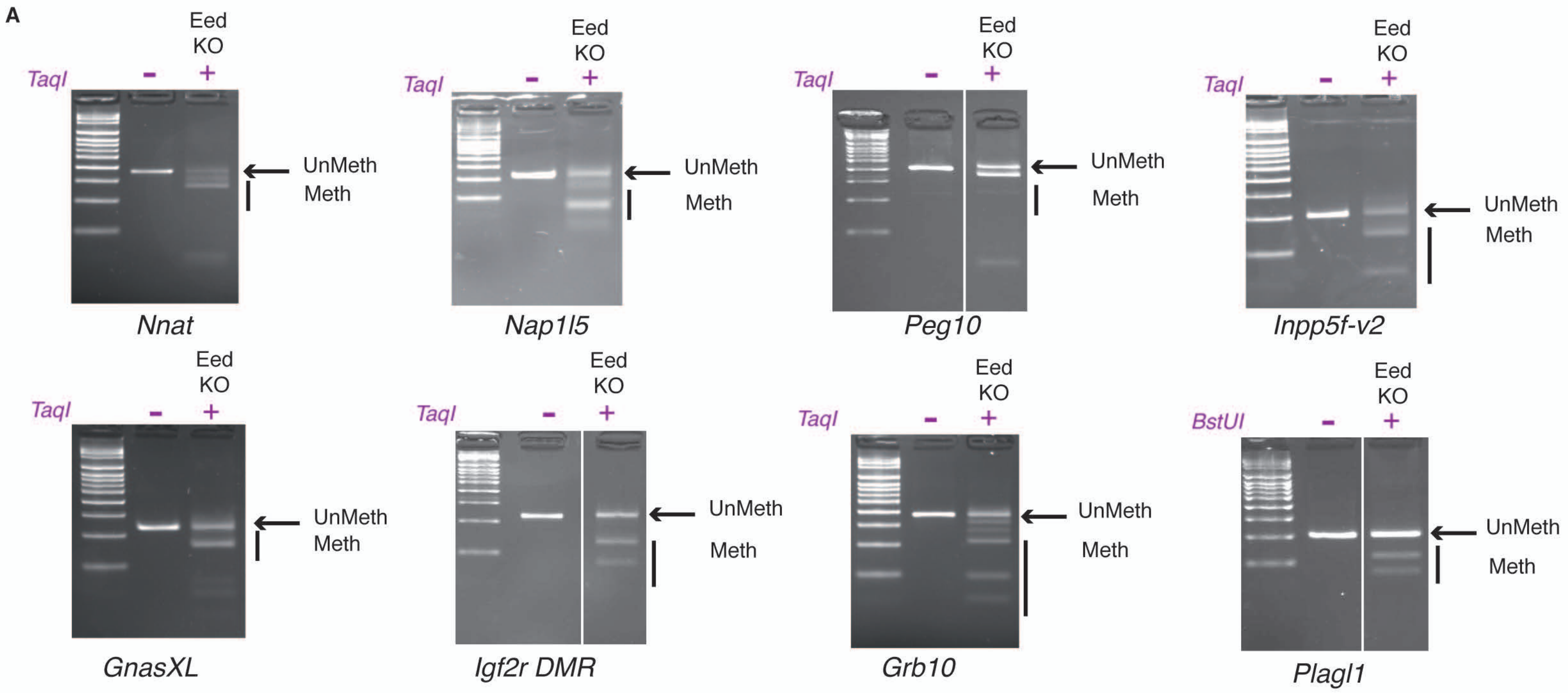
A
TaqI
Eed KO
-
+
UnMeth
Meth
Nnat
Nap1l5
Peg10
Inpp5f-v2
GnasXL
Igf2r DMR
Grb10
BstUI
Plagl1

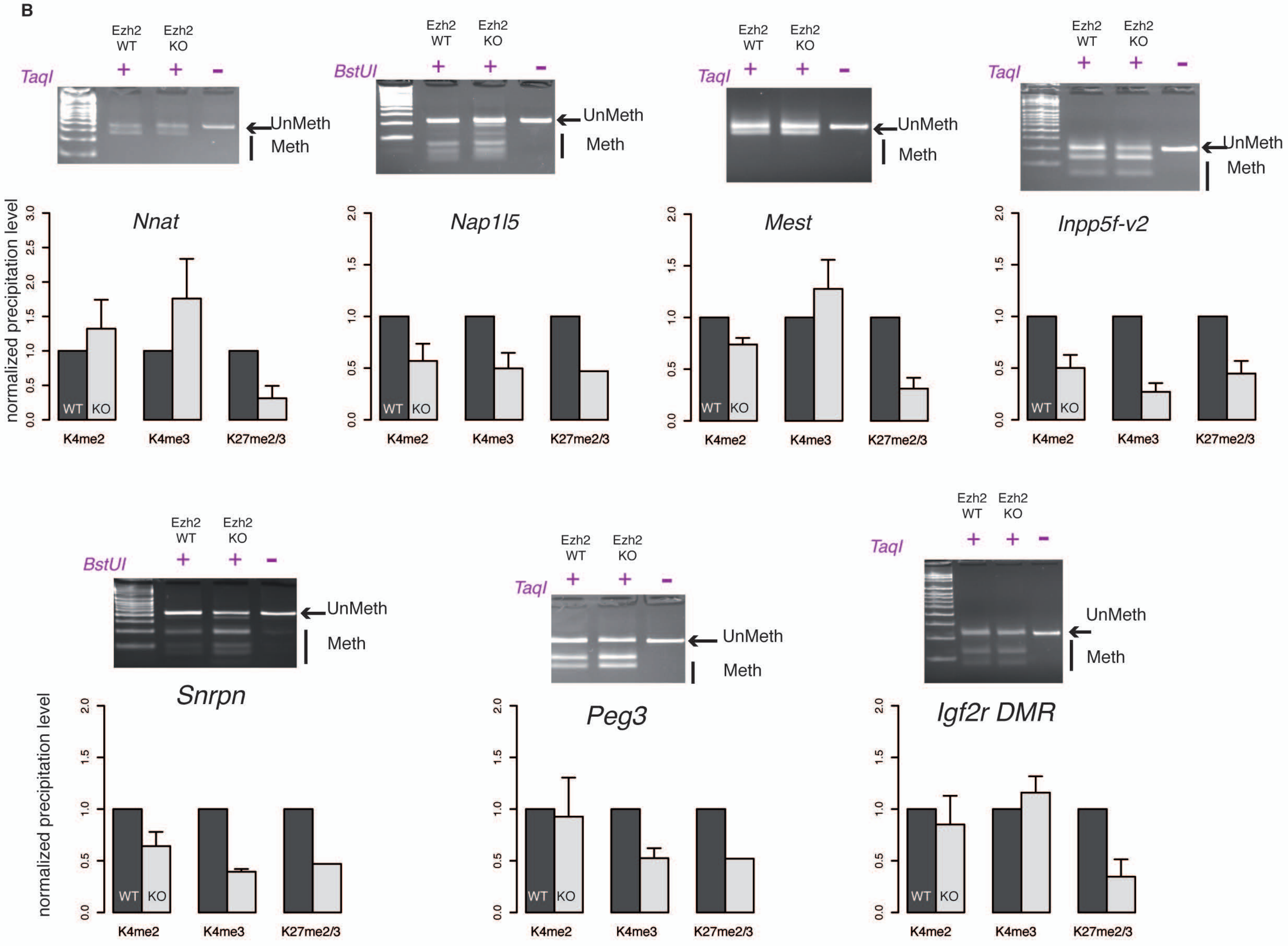
B
TaqI
BstUI
Ezh2 WT
Ezh2 KO
+
-
UnMeth
Meth
normalized precipitation level
Nnat
Nap1l5
Mest
Inpp5f-v2
Snrpn
Peg3
Igf2r DMR
WT
KO
K4me2
K4me3
K27me2/3
0.0
0.5
1.0
1.5
2.0
2.5
3.0

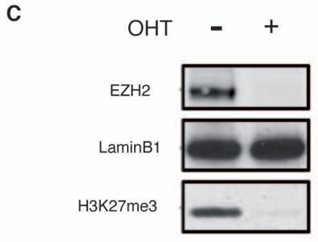
C
OHT
-
+
EZH2
LaminB1
H3K27me3

Supp.Fig 8

Supplementary Figure S8: Epigenetic signature at ICRs in PRC2-deficient cell lines

A) Representative data obtained using the bisulfite-based approach COBRA in *Eed* $^{-/-}$ ES cells for the indicated ICRs. The enzyme used for the digestion and the expected position of the obtained methylated (Meth.) and unmethylated (UnMeth.) digestion products are indicated. The presence of both methylated and unmethylated molecules suggests that the DNA methylation pattern is not altered at ICR regions in EED-deficient cells.

B) ICRs are depleted for H3K27me3 in *Ezh2* $^{-/-}$ iMEF cells. The upper panel show representative data obtained using the bisulfite-based approach COBRA in *Ezh2* $^{-/-}$ iMEF cells for the indicated ICRs. In the lower panel, deposition of the indicated histone modifications was evaluated in the same ICRs, following native ChIP. To ascertain that H3K27me2 and H3K27me3, which are both associated with repression (Ferrari et al., 2014), are affected at ICRs in *Ezh2* $^{-/-}$ iMEFs, we used an antibody raised against these two modifications (Active Motif, ref 39535, Clone 7B11). The precipitation level was normalized to the level obtained in wild type iMEF cells. When data were obtained from two independent ChIP experiments done using the same chromatin preparation, the standard deviation was not determined.

C) Global H3K27me3 reduction in *Ezh2* $^{-/-}$ iMEF cells. Detail of western blot analysis in iMEF cells before (-) and after (+) treatment with 4-Hydroxytamoxifen (OHT).

Supp.Fig 9

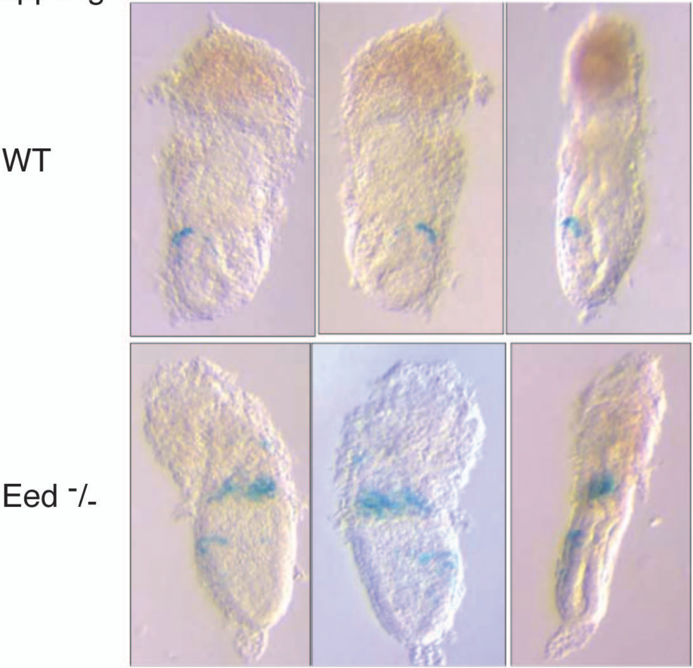

Supplementary Figure S9: EED deficiency has a limited impact on paternal *Grb10* expression in E6.5 conceptuses.

Embryos from a cross between an *Eed*$^{-/+}$ female and an *Eed*$^{-/+}$ male bearing a lacZ insertion in *Grb10* exon 7 (referred to as Grb10XC302) were collected at 6.5 d.p.c., genotyped and stained with X-Gal. Reproduced from (Sanz et al., 2008), with permission from EMBO J.

Suppl. Table S1

		ChIP analysis			Bisulfite analysis			Transcripts analysis		
ICR	**Associated transcript**	**Primers 5' -> 3'**	**SNP B6/JF1**	**SNP mm9 position**	**Primers 5' -> 3'**	**SNP B6/JF1* (given following bisulfite conversion)**	**SNP mm9 position**	**Primers 5' -> 3'**	**SNP B6/JF1**	**SNP mm9 position**
Nnat	*Nnat*	AGGTGAGTATGTACCCGGGCTTT AGCGGGTATTTCTTACCGCGTTG	A/G	chr2:157,386,111 (rs27338077)	TGTTGTTGTAGGTGAGTATG TTTCACAACACACAAATACCC	A/G	chr2:157,386,111 (rs27338077)	TTCTGATCTGGACCAAGTCG TTAACCCTCTTCCTCCACCAC	G/A T/C	chr2:157,387,678 (rs27338074) chr2:157,387,807 (rs27338072)
Peg10	*Peg10*	CGCTTCAGCGTACGAACGAGCA GTGCCGCAGTTTGTAGCGCATT	C/T G/T T/C	chr6:4,698,341 chr6:4,698,351 chr6:4,698,384	GAATTTGTGAAYGGGGTGAA CTCCACTACCATAAACAAAAATTAC	G/T T/C T/A	chr6:4,698,351 chr6:4,698,384 chr6:4,698,413	CCTAGGAATTCGTTGGCTGA GATGCATATGCGGATGGAC	A/T	chr6:4,705,839 (rs32465148)
Nap1l5	*Nap1l5*	TGCGCAACCACCAGACCACTGC AGATATCGTTGTACTTCTTCT	G/A	chr6:58,856,871 (rs49797894)	GTAAATAAGTTTAGTTGAGT ACAAACTCTCCATAAAATCT	G/A	chr6:58,856,871 (rs49797894)	TGCGCAACCACCAGACCACTGC AGATATCGTTGTACTTCTTCT	G/A	chr6:58,856,871 (rs49797894)
Inpp5f-V2	*Inpp5f-V2*	TTCCTGCCTGCGCTCTCAGC GCCGGTGGAGCTGTTGGGTG	T/C C/T T/G C/T	chr7:135,831,638 (rs50368586) chr7:135,831,813 (rs31346795) chr7:135,831,826 (rs31752757) chr7:135.831.831	TGATGGGTAGAGGGTTGTTA CTCAACCACCTCATTTACCA	A/G	chr7:135,831,638 (rs50368586)	CAGGATGGAAGTGACACTGTAG CCACATAGTAGGCAGCGTTAG	G/T	chr7:135,807,616 (rs49202299)
Grb10	*Grb10**	TCAGGGTTGCCATGAGAACCAG CGCTAAGCGAAGCAACACAGCCT	A/G	chr11:11,926,748	AGAGAAGATATGTTGAAGTTAT TCTACCACTTAACTAAAAACAA	G/A G/A	chr11:11,925,631 chr11:11,925,564	GTCAATTCCCTGGAAGCTGAGAA CTGGTTGGCTTCTTTGTTGTG	G/A	chr11:11,887,647
Plagl1	*Plagl1*	TTGGCCTCTGGCTTACAAAG GTGACTCATCGGCTGTATGC	T/C	chr10:12,810,302 (rs33581138)	ATTTTGAATTTGGGTGTTTT AAACACAAATCACCTCTTCC	A/G	chr10:12,811,102 (rs29364824)	GGCTTTCCTGCTCTCACAGA ATGGCCTTTGGTTCTCACAC	C/T	chr10:12,844,715 (rs29342169)
GnasXL	*GnasXL*	AATGTCAGCCTCTGCTAGGG GTCAGCAACCTGGATCTCG	C/A	chr2:174,125,210 (rs6300782)	GGTTTGGGGAGTTAGGTTAT TACTTATCAAACCAAACAATC	T/A	chr2:174,125,210 (rs6300782)	AACTGGAGGAGGAGAAGATGG GCCACAATGGTTTCAATGG	/	
Igf2r-DMR	*Airn*	GGAGGATTCTGCAGATGAGG GCGTAGGGGAACCTTTGAG	A/G	chr17:12,934,366	ATTTTGTAGATGAGGGTAGGATT AAATTTTCTTATAACCCAAAAATCT	A/G	chr17:12,934,366			
KV-DMR	*Kcnq1ot1*	GCCAAGTGGATCGCGCCAAG CGGATCACTTGAGCACTAC	A/G	chr7:150,481,965 (rs33827265)	GTGTGATYGTTTTTTGTATGGT CTAAACAAAAAAACTCTCCAA	T/G T/C T/TT G/C	chr7:150,482,175 chr7:150,481,965 (rs33827265) chr7:150,481,872 chr7:150.481.863 (rs33838855)	TTTCTCTGCATGGTCCTTCC TTGAGCAAAGCACACTGAGG	C/G	chr7:150,482,175
Snrpn	*Snrpn*	AGGTTGTGACTGGGAATCCTG GCGGCAACAGAACTTCT	G/A A/G	chr7:67,149,670 (rs49517599) chr7:67,149,505 (rs48289421)	ATTGGTGAGTAATTTTTTGGA ACAAAACTCCTACATCCTAAAA	G/A A/G A/G	chr7:67,149,670 (rs49517599) chr7:67,149,505 (rs48289421) chr7:67,149,480 (rs50419566)	ATGCAAAACAGCCAGAACG ACACGAGCAATGCCAGTATC	A/C	chr7:67,131,688 (rs51293023)
Peg13	*Peg13*	CTCTGTGCTAGCGTCTCCAG AGGCACAGAAAAAGCCCAGA	A/G G/A	chr15:72,640,049 (rs31423566) chr15:72,640,057				CTCTGTGCTAGCGTCTCCAG AGGCACAGAAAAAGCCCAGA	A/G G/A	chr15:72,640,049 (rs31423566) chr15:72,640,057
Mest	*Mest*	GGCATTAACACATGGGAAGG CCGACTTTTAAAGCCCACTG	T/C	chr6:30,688,000	GAAGTAGAGAGGAGTAAGTAGGTAT AACTTTCTTCACTAAAATCTAAAATTC	A/G	chr6:30,688,000	GATTCGCAACAATGACGGCA ATCCAGAATCGACACTGTGG	T/C	chr6:30,695,854
Peg3	*Peg3*	GCCTTGTCAGTTACCCTTGG GAGAAGCGGAGAGATGTCCA	C/T	chr7:6,682,875 (rs45678166)	TTGATAATAGTAGTTTGATTGGTAGGGTGT ATCTACAACCTTATCAATTACCCTTAAAAA	G/A	chr7:6,682,875 (rs45678166)	CCTGAGGCCAAAAAGCCATC CTTGGAGGAGGACGCTCGTT	C/T T/C G/A	chr7:6,664,405 chr7:6,664,399 (rs50075878) chr7:6,664,341 (rs50587768)
U2af1-rs1	*U2af1-rs1*	CGGATAATCGCGGATAATTG TCGGAGGTACGGATGGTCT	C/G A/C	chr11:22,872,443 (rs26846195) chr11:22,872,498 (rs26846194)				CACGGAGGCTGGCCTTAAA CCGCGATTATCCGTGGTACA	C/T G/A	chr11:22,872,276 chr11:22,872,288 (rs26846196)
Impact	*Impact*	GCCCCGCATCTCTTAACAT TTATGTGACAATGCGGCAAA	G/C	chr18:13,132,215				ATTTATGGCGAGGAGTGGTG AGTGTCCATTTGGGGTCATC	A/G	chr18:13,133,281 (rs31056582)

Supp. Table S2

ChIP analysis

Genomic region	Primers 5' -> 3'
Rpl30 promoter	AGCACGCCCAAGACAACGTCA TGTGCGGTAGTTGGTTGCTA
IAP	TATGCCGAGGGTGGTTCTCTA TGCGGCAAAACTTTATTGCTT
HoxA3 promoter	CATCCGCTCATACCAAGCTTCTGA GCAGGGAGGTAATTGCTGTGGTTT
HoxD8 promoter	CAGTCTCTGGCAGTTCTTT CCTGTCCTGTGCTTAACG

Transcript analysis

Transcript	Primers 5' -> 3'
Ppia	GTGGTCTTTGGGAAGGTGAA TTACAGGACATTGCGAGCAG
Rpl30	AGTCTCTGGAGTCGATCAACT AGCCAGTGTGCATACTCTGTAG
Gapdh	ACAGTCCATGCCATCACTGCC GCCTGCTTCACCACCTTCTTG
Tbp	GCGATTTGCTGCAGTCATCA CAGCTCCCCACCATGTTCTG
Arbp	TGCCACACTCCATCATCAAT CGAAGAGACCGAATCCCATA

Supp. Table S3

antibody	H3K4me2	H3K4me2	H3K4me3	H3K9Ac	H3K9me3	H3K27me3
Provider	**Abcam**	**Millipore**	**Diagenode**	**Millipore**	**Millipore**	**Millipore**
Reference	Ab32356	Milli 07-030	Diagenode 030-050	Milli 06-942	Milli 07-442	Milli 07-449
lots	gr39844-3 gr84702-1 947550 GR39894-3	2309072 2089140	1	31636	JBC1865906 JBC1361819 2043528 dam 1739170	JBC1873477 1959680 JBC1764447

References:

1. Bunch,H., Zheng,X., Burkholder,A., Dillon,S.T., Motola,S., Birrane,G., Ebmeier,C.C., Levine,S., Fargo,D., Hu,G., Taatjes,D.J., Calderwood,S.K. (2014) TRIM28 regulates RNA polymerase II promoter-proximal pausing and pause release. *Nat Struct Mol Biol*; 21:876-83.

2. Di Cerbo,V., Mohn,F., Ryan,D.P., Montellier,E., Kacem,S., Tropberger,P., Kallis,E., Holzner,M., Hoerner,L., Feldmann,A., Richter,F.M., Bannister,A.J., Mittler,G., Michaelis,J., Khochbin,S., Feil,R., Schuebeler,D., Owen-Hughes,T., Daujat,S., Schneider,R. (2014) Acetylation of histone H3 at lysine 64 regulates nucleosome dynamics and facilitates transcription. *Elife* 25;3:e01632

3. Ferrari KJ, Scelfo A, Jammula S, Cuomo A, Barozzi I, Stützer A, Fischle W, Bonaldi T, Pasini D. (2014) Polycomb-dependent H3K27me1 and H3K27me2 regulate active transcription and enhancer fidelity. *Mol Cell.* 53:49-62.

4. Sanz,L.A., Chamberlain,S., Sabourin,J.C., Henckel,A., Magnuson,T., Hugnot,J.P., Feil,R., Arnaud,P. (2008) A mono-allelic bivalent chromatin domain controls tissue-specific imprinting at Grb10. *EMBO J* 27:2523-32